MECHANICAL BEHAVIOR OF RUBBER AT HIGH STRAIN RATES

C. M. ROLAND*

CHEMISTRY DIVISION, CODE 6120
NAVAL RESEARCH LABORATORY
WASHINGTON, DC 20375-5342

ABSTRACT

Methods to obtain the mechanical response of rubber at high rates of strain are reviewed. These techniques include the extrapolation of low strain, low strain rate data, the limitations of which are discussed, extrapolations to elevated hydrostatic pressure, and direct determinations using split Hopkinson bar and drop weight testers, as well as miscellaneous methods. Some applications involving rubber at strain rates sufficient to induce a transition to the glassy state are described.

CONTENTS

I. INTRODUCTION

This review discusses the mechanical behavior of rubber at high strain rates, a topic that taken to the extreme is a contradiction in terms. Rubber refers to any amorphous, flexible chain high-polymer having a sub-ambient glass transition temperature, T_g. Since effectively T_g is defined as the temperature at which the material response (*i.e.*, the local segmental dynamics) becomes significantly slower than the experimental time scale (*i.e.,* Deborah number >> 1), the glass transition is rate-dependent. This means rubber being strained very rapidly can behave as a glass, so that the rubbery state may not persist at high strain rates. In fact, as discussed herein in Section IV, the transition of rubber to a glass underlies some applications for rapidly strained rubber. The other phase change induced by the deformation of rubber, strain-induced crystallization, is also affected by high strain rates. In high speed tension tests on natural rubber, Mitchell and Meier[1] found that strain-crystallization required 45 to 65 ms at ambient temperature. This result was corroborated in subsequent studies by Glaser and Eirich.[2] Lake *et al.*[3] reported that when

* Ph: 220-767-1719; Fax: 202-767-0594; email: roland@nrl.nay.mil

crack growth rates in natural rubber exceed about 1 cm/s, there is insufficient time for strain crystallization at the crack tip.

Accurate testing of rubber at high rates of strain can be difficult. For linear measurements (modulus independent of strain amplitude), dynamic mechanical spectroscopy provides characterization over a wide range of rates (~ 5 decades); however, the upper frequency is usually only 10 – 100 Hz. Specialized instruments extend the range to ~10^4 Hz[4] but these are not in common use. Atomic force microscopy ("nanoindenters") yield indirectly the mechanical properties of surfaces,[5,6] and these can be operated at rates as high as 1 MHz.[7,8] However, the strains are low and only the surface is probed.

The frequency range of conventional mechanical spectroscopy can be extended by invoking the time-temperature superposition principle.[9] First demonstrated by Tobolsky and Andrews,[10] this method is illustrated in Figures 1 and 2, which show respectively strain to failure[11] and friction[12] measurements on rubber at high rates and velocities. The data obtained at various temperatures superpose to form a master curve; however, at the lowest temperatures (highest reduced rates) there is no overlap of measurements at different temperatures. Thus, while there is no indication of a breakdown of the superposition principle, the validity of the master curves for high reduced frequencies cannot be judged from the data *per se*. The curves were constructed assuming superpositioning to be valid, which relies in turn on one of two assumptions: that the molecular motions relevant to the property being tested remain the same at all test temperatures or if not, that all modes have the same temperature dependence.

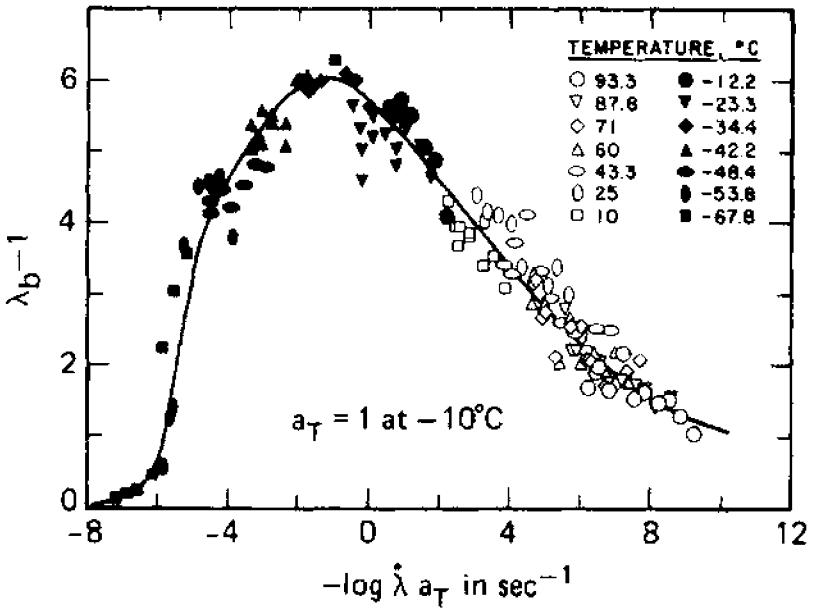

FIG. 1. – The elongation at break versus negative logarithm of the reduced extension rate for an SBR. The actual tests covered as much as 3 decades in extension rate.[11]

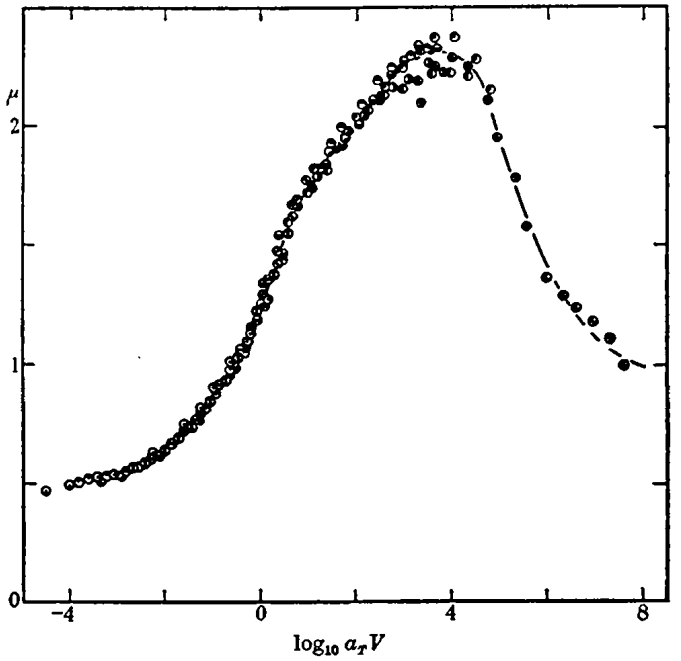

FIG. 2. – Friction coefficient of natural rubber on silicon carbide paper versus the log of the reduced sliding velocity in cm/s. The reference temperature was 20 °C and the actual temperatures were -58 to 90 °C. The material was isomerized to suppress crystallization.[12]

In this review we scrutinize the practice of time-temperature shifting to characterize the mechanical properties of rubber at high rates, and also discuss approaches to predict the response at elevated pressure for rates beyond those actually measured. Various methods of directly testing rubber at high strains and high strain rates are reviewed. Finally, we describe some applications involving rapidly deformed rubber. The focus herein is on the stress/strain behavior rather than the failure properties of elastomers at high rates of strain.

II. EXTRAPOLATION OF LOW STRAIN RATE MEASUREMENTS

A. TIME-TEMPERATURE SUPERPOSITIONING

In Figure 3 are shown master curves of the dynamic shear moduli for uncrosslinked *cis*-1,4-polyisoprene (synthetic natural rubber, PI).[13] There is apparently good superpositioning of the data, which were measured over a range of temperatures from T_g (= -71 °C) to 80 °C. Vertical arrows on the figure denote the terminal relaxation time (onset of flow), the longest Rouse relaxation time (onset of entanglement constraints demarcating the rubbery plateau), and the local segmental relaxation time (involving intramolecularly correlated motion of a few backbone bonds[14,15]). As frequency increases, successively shorter length scales are involved in the underlying motions, and eventually no polymeric modes contribute to the response. Note that in Figure 3, measurements at only one temperature are shown in the transition zone; thus, any breakdown in time-temperature superpositioning cannot be detected. Horizontal shifting of the (relatively featureless) curves will cause their overlap, particularly with the usual small adjustments in ordinate values. However, if one compares the loss tangent, tan δ, for these same data (Figure 3 inset), there is a marked change in shape with temperature, revealing a breakdown of superpositioning in the transition zone. This breakdown is due to the difference in temperature dependence

of the local segmental motion and the chain (polymeric) dynamics, a phenomenon first discovered in polystyrene more than 40 years ago.[16,17] (For unentangled linear polymers, these chain motions are described as Rouse modes; for higher molecular weight polymers, the long-time processes include both Rouse modes involving chain units between entanglements and the terminal chain modes described, for example, by reptation models.[9,17,18]) Clearly this thermorheological complexity can only be observed by measurements extending over a broad enough range of frequencies. If isothermal data are taken over only a few decades, results can be combined apparently successfully to yield master curves, as shown in Figure 3. Of course, for spectroscopies that probe only the segmental motions, such as dielectric relaxation of "type-B" dipoles (transverse to polymer chain so that the normal modes are dielectrically inactive;), any departure from time-temperature equivalence becomes moot.

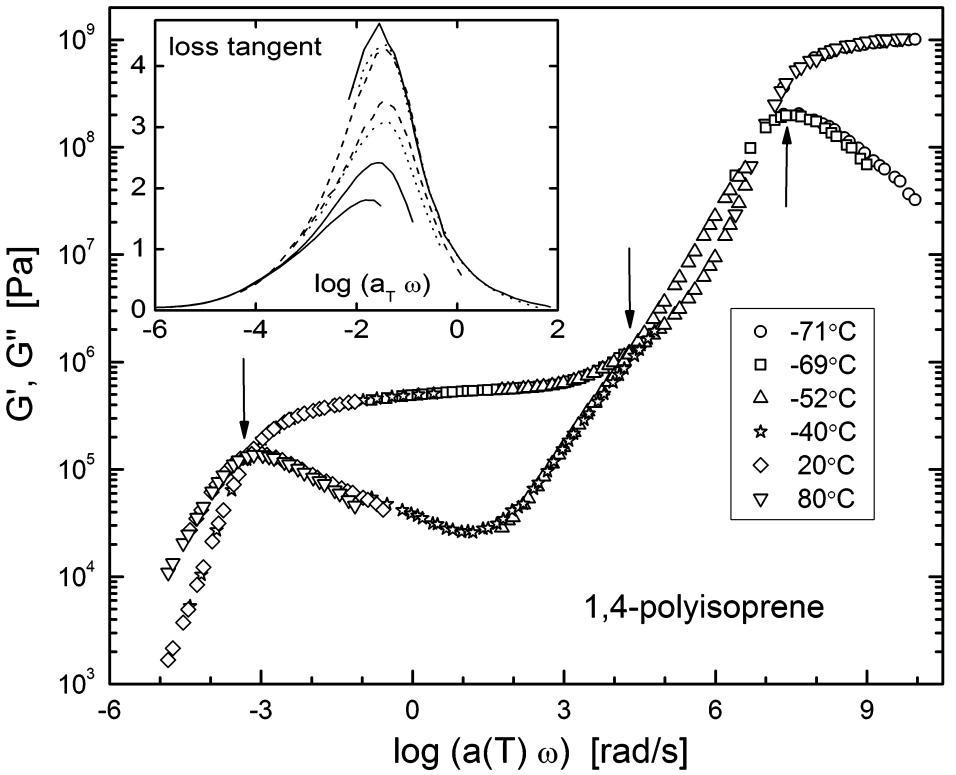

FIG. 3. – Master curves for the dynamic storage and loss moduli of PI (M_w=500 kg/mol) at a reference temperature = -10 °C.[13] The arrows denote (from left to right) the frequency associated with the terminal chain mode (onset of flow), the slowest Rouse mode (onset of entanglement effects) and local segmental relaxation (onset of the glass transition). The inset shows the loss tangent over a temperature range from -48 °C to -66 °C, corresponding to the transition zone. In the master curves, data measured at only one temperature is used for the transition zone in order to obtain ostensibly satisfactory superpositioning.

PI has type-A dipoles (parallel to the backbone) and thus dielectric spectroscopy can be used to probe the motions of the chain end-to-end vector. By combining mechanical and dielectric results, shift factors, a(T), for both modes can be obtained over a wide, overlapping range, and the stronger T-dependence of the local modes is made evident (Figure 4). In the more usual experiment, the segmental mode is measured at low temperatures and the chain modes at high temperatures, with the collected shift factors forming a smooth, continuous curve; however, enor-

mous errors would result from extrapolation using such results. Similar behavior to Figure 4 is also seen in broadband dielectric measurements on lower molecular weight PI.[19]

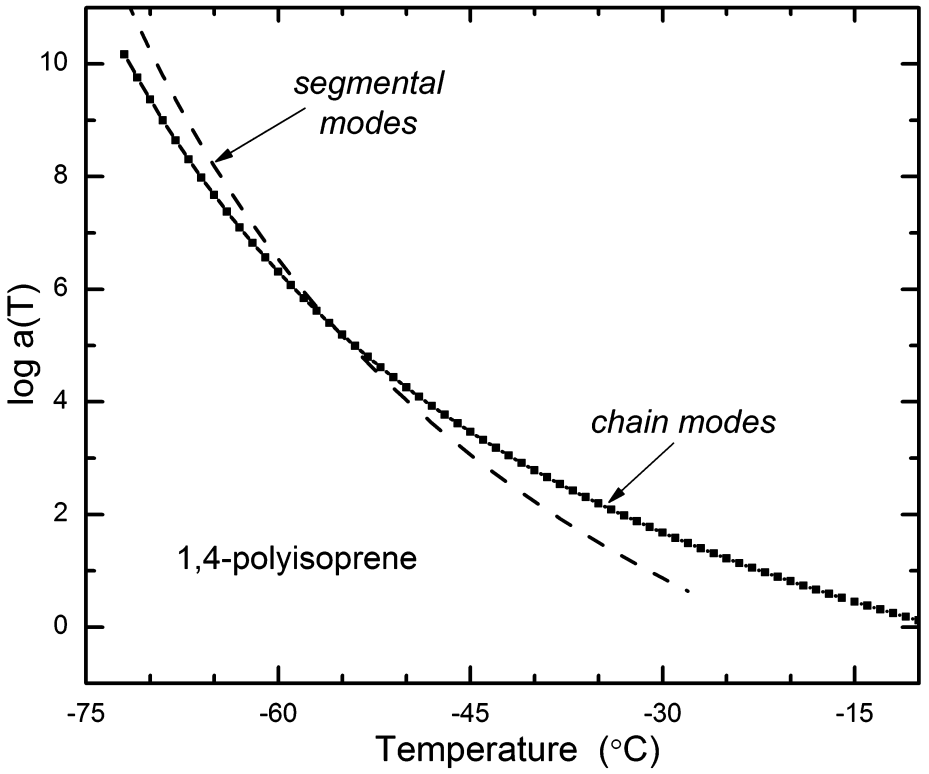

FIG. 4. – Time/temperature shift factors for PI from mechanical and dielectric spectroscopies.[13] Typically segmental modes are measured at low T and chain modes at high T, leading to large extrapolation errors.

The phenomenon shown for PI is completely general. For every polymer for which sufficient measurements have been made, the local and chain modes exhibit different time-temperature shift factors. This is shown in Figure 5 for atactic polypropylene,[20] wherein results from mechanical, dielectric, light scattering and NMR measurements are combined to yield relaxation times, τ, and a(T) encompassing more than 14 decades of frequency. The timescale for the segmental dynamics changes more with a given change in temperature than do the chain modes.

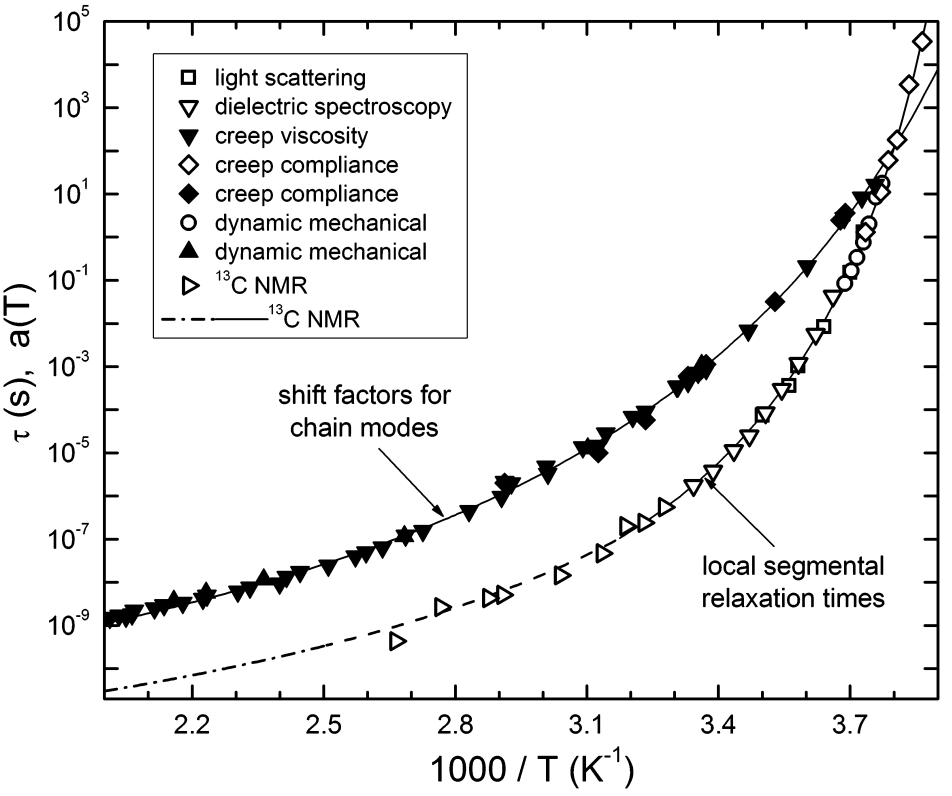

FIG. 5. – Local segmental relaxation times and time/temperature shift factors for atactic polypropylene determined by the indicated methods.[20] The ordinate values for a(T) of the chain modes are shifted arbitrarily (the relaxation times for polymeric modes are always larger than the segmental relaxation times when compared at the same temperature).

Although the breakdown of time-temperature superpositioning is usually seen as a decrease in the height of the loss tangent peak with increasing temperature or poor overlap in the transition zone of different isothermal data sets, for polyisobutylene (PIB) the effect is more dramatic: there is a large change in the shape of the loss tangent peak with changing temperature (Figure 6).[21] This peculiar behavior is believed to arise from the viscoelastic contribution of "sub-Rouse" modes,[17,22] which are chain segments too short to exhibit Gaussian statistics (and so cannot be regarded as Rouse modes) but too long to participate in the segmental dynamics associated with structural relaxation. It is ironic that one of the most marked examples of deviation from the superposition principle is seen in the polymer largely responsible for the universal acceptance of the very concept.[23]

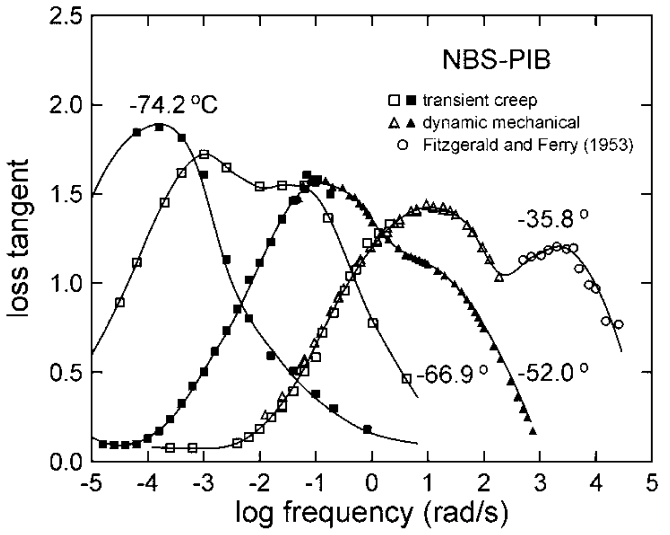

FIG. 6. – Mechanical loss tangent for polyisobutylene measured at different temperatures.[21] The two peaks reflect two viscoelastic mechanisms having different temperature dependences. The particular sample was the same as that used in Reference 23.

B. TEMPERATURE-VOLUME SUPERPOSITIONING

The previous section describes the problems associated with invoking an equivalence between time and temperature effects in order to extrapolate dynamic properties to frequencies beyond those actually measured. An analogous approach can be used to generate master curves of moduli measured at different pressures[9] but the data are scarce and interpretation of the results problematic. Dielectric measurements at elevated pressure are much more common, since the absence of moving parts facilitates immersion of the sample in a pressurizing fluid.[24] From such data it has been found that local segmental relaxation times can be superposed when plotted as a function of temperature times the specific volume (V ≡ inverse of mass density), with the latter raised to a power of γ.[25-27] The exponent γ is a material constant, usually determined by empirical superpositioning of relaxation times measured at various combinations of temperature and pressure and plotted versus TV^{γ}. The exponent can be related to the intermolecular repulsive potential, leading to a connection of γ to the Grüneisen parameter and to the pressure coefficient of T_g.[28] If the relaxation times are expressed as a function of the configurational entropy, an expression can be derived showing that τ will be a function of TV^{γ}.[29] This seems to support an entropy basis for the arrest of molecular motions associated with the glass transition. Results for several rubbers are shown in Figure 7.[24,26] Analogous behavior is observed for simple (small molecule) liquids in the supercooled regime; their structural relaxation properties, involving molecular reorientations and translations, parallel the local segmental dynamics of polymers.[24] In fact, it is not possible to distinguish a polymer from a molecular liquid based on relaxation measurements near T_g.

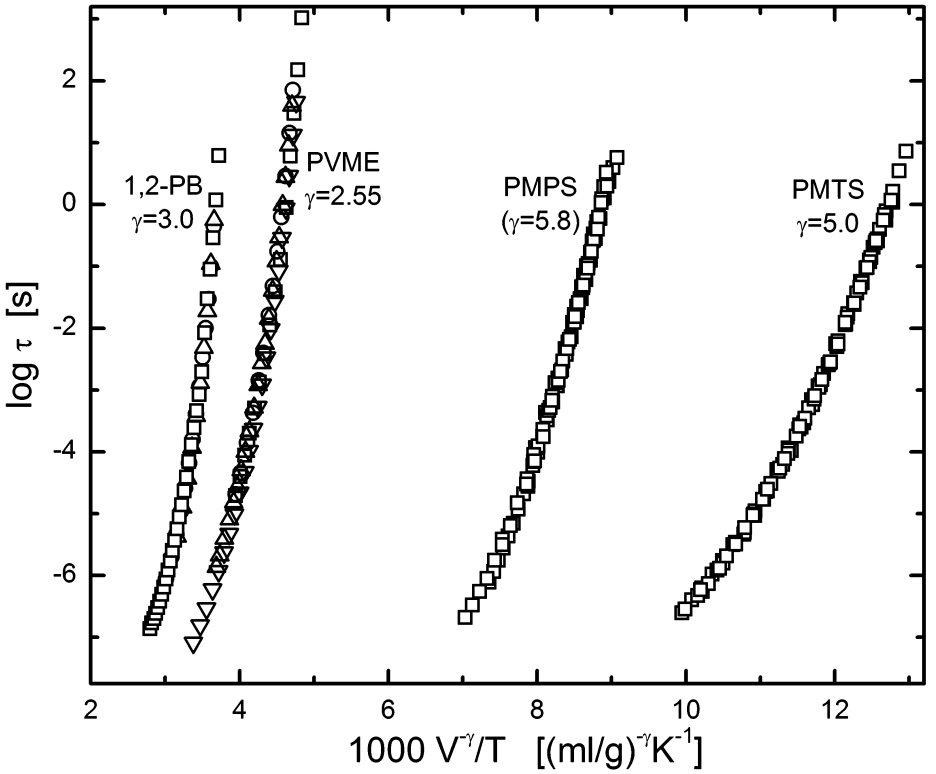

FIG. 7. – Segmental relaxation times measured by dielectric spectroscopy for 1,2-polybutadiene (1,2-PB), polyvinylmethylether (PVME), polymethylphenysiloxane (PMPS), and polymethyltolylsiloxane (PMTS) versus the reciprocal of the product of temperature times specific volume with the latter raised to the indicated power. The different symbols for each rubber correspond to different measurement conditions: varying temperature at 0.1 MPa (□) and varying pressure at different temperatures.

As mentioned above, type-A polymers have a dipole moment parallel to the backbone and thus exhibit dielectrically-active normal modes, reflecting global motion of the chain. The chain modes not only have a different dependence on temperature than the local segmental modes (Figures 4 - 6), but also differ in pressure- and volume-dependences.[30,31] Interestingly, however, the normal mode relaxation times superpose when plotted versus the same function TV^{γ} using the same value of γ. Results are shown in Figure 8 for polyoxybutylene,[32] Figure 9 for PI,[33] and Figure 10 for polypropyleneglycol.[33] Note that in each case, the variation of τ with TV^{γ} is steeper for the segmental mode than for the normal mode, consistent with the stronger T-, P-, and V-dependences of the former.

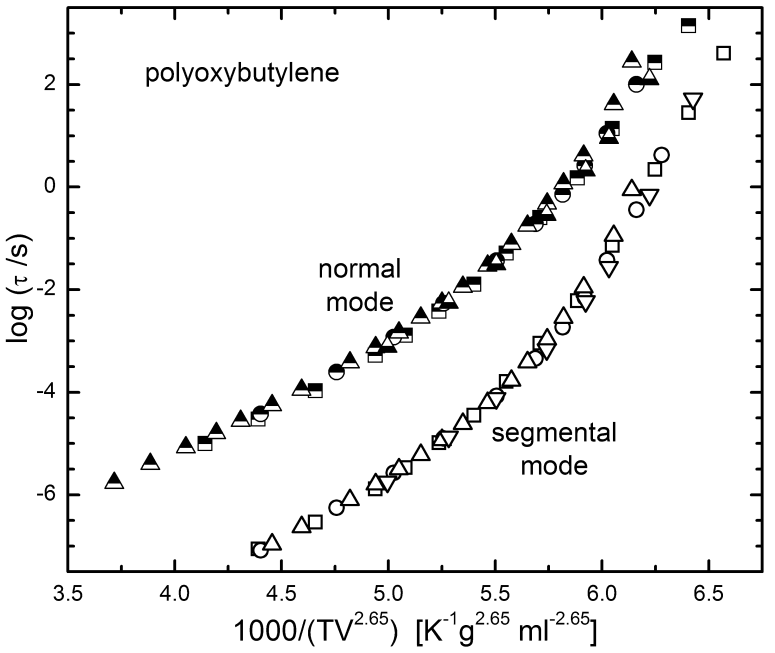

FIG. 8. – Scaled plots of the dielectric relaxation times for polyoxybutylene (M_w = 5.3 kg/mol) measured at various conditions of T and P.[32] Although the same value of γ (= 2.65) superposes both the local modes and the chain modes, the latter have a weaker dependence on TV^{γ}.

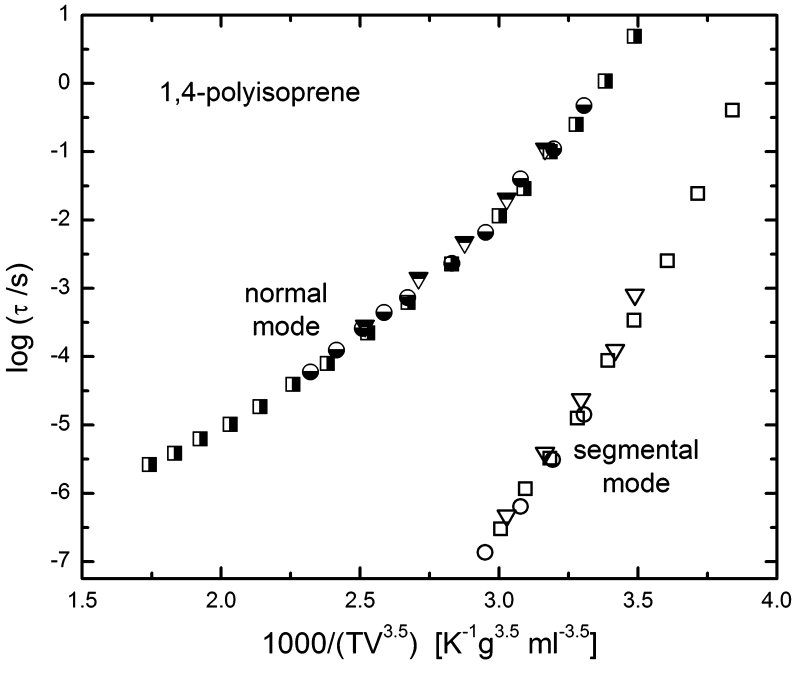

FIG. 9. – Scaled plots of the dielectric relaxation times for 1,4-polyisoprene (M_w = 11.1 kg/mol) measured at various conditions of T and P[33] (original data from Floudas *et al.*)[30] Although the same value of γ (= 3.5) superposes both the local modes and the chain modes, the latter have a weaker dependence on TV^{γ}.

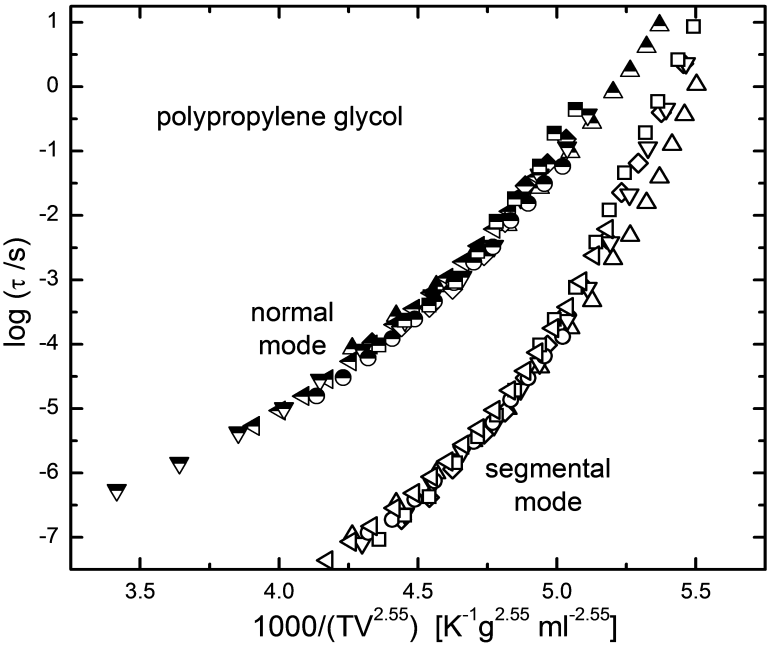

FIG. 10. – Scaled plots of the dielectric relaxation times for polypropyleneglycol (M_w = 4.0 kg/mol) measured at various conditions of T and P.[33] Although the same value of γ (= 2.55) superposes both the local modes and the chain modes, the latter have a weaker dependence on TV^{γ}.

This scaling of relaxation times is not useful for extrapolating beyond frequencies actually measured; however, since data at elevated pressure can usually be obtained only over a limited frequency range,[24,34] scaling enables extrapolation of high pressure data to the frequencies measured at ambient pressure. Moreover, the scaling exponent γ can be obtained directly from pressure-volume-temperature data.[28] This means that the variation of relaxation times with P and V can be determined without carrying out any relaxation measurements beyond ambient pressure. Since the deformation of rubber at very high strain rates often involves high pressures (*e.g.*, the production of shock waves in rubber), characterization of the mechanical response may entail quantifying the effect of pressure.

C. TEMPERATURE-PRESSURE SUPERPOSITIONING

Sometimes the local segmental relaxation function (*i.e.*, time-dependence of modulus or dielectric loss) does not change shape when pressure is varied at fixed temperature; an example is polymethylphenylsiloxane, shown in Figure 11.[35] More usually there is some broadening as pressure increases, similar to the increase in breadth of the relaxation function with isobaric cooling towards T_g. The relaxation time determined for a given material at ambient pressure can be maintained constant with increases of both temperature and pressure; that is, various combinations of P and T can be found for which the frequency of the maximum in the mechanical or dielectric loss remains the same.

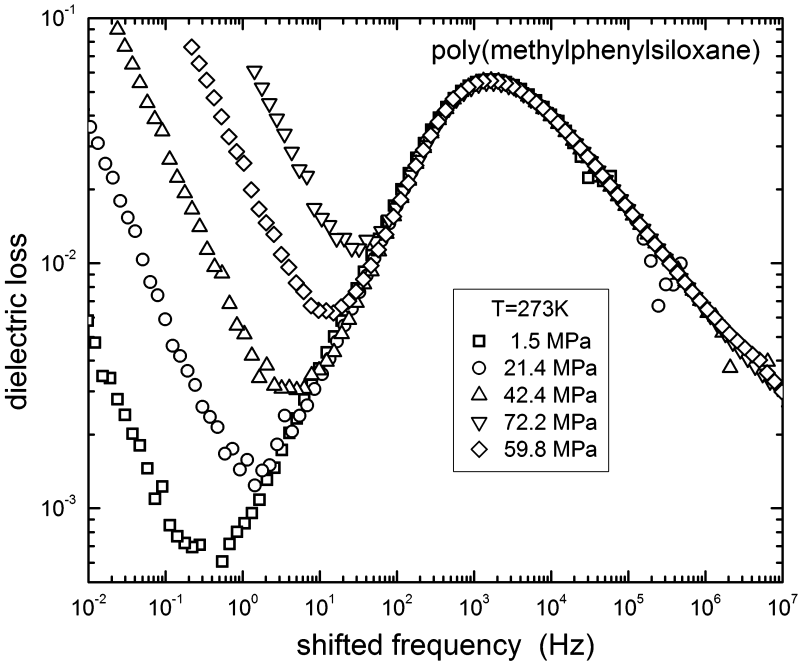

FIG. 11. – Dielectric loss curves for segmental relaxation of PMPS measured at the indicated pressures.[35] The data were shifted to superimpose on the curve for P = 42.4 MPa. The steep rise toward lower frequency is due to conductivity from mobile ions within the polymer.

Recently it was discovered that at a fixed value of local segmental (or structural) relaxation time, the relaxation function is constant, independent of thermodynamic conditions.[36-38] This means that T-P superpositioning applies to the dispersion in the mechanical or dielectric loss. Examples are shown in Figure 12 for 1,2-polybutadiene[39] and 13 for poly(ethyl-co-vinyl acetate).[40] The only exception to this behavior appears to be strongly hydrogen-bonded liquids, for which changes in T and P change the material itself (*i.e.*, the degree of H-bonding), not just the dynamics.[36] The fact that the shape of the relaxation function depends solely on the relaxation time means that measurements at ambient pressure suffice to characterize the local segmental function for any T,P combination. The value of τ(T,P) can be determined by invoking the scaling procedure described in the preceding section, in combination with the equation of state (PVT relation).

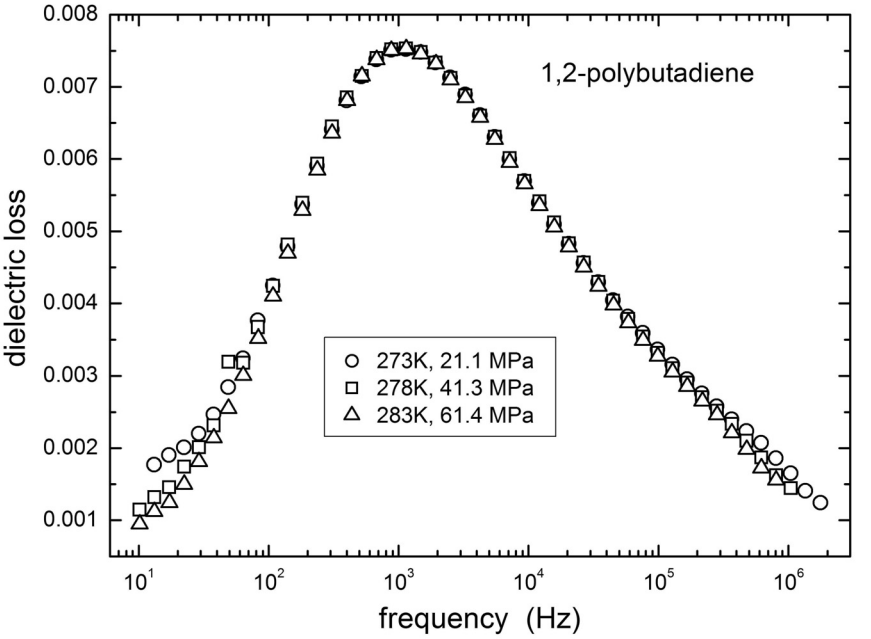

FIG. 12. – Dielectric loss curves for 1,2-polybutadiene[39] at the indicated combinations of temperature and pressure demonstrating the invariance of the dispersion at constant value of the local segmental relaxation time. The ordinate scale for each curve has been shifted slightly to make the peaks coincide at their maxima.

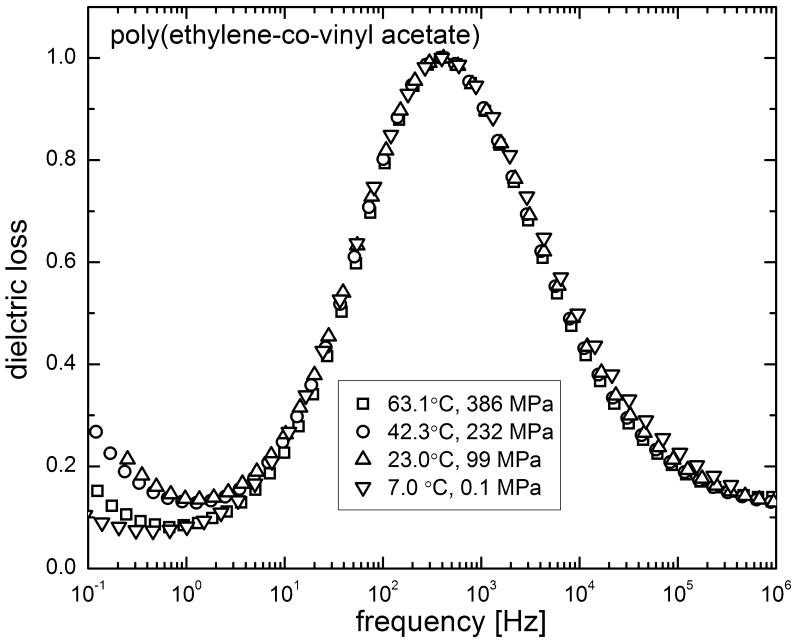

FIG. 13. – Dielectric loss curves for a random copolymer of ethylene and vinyl acetate (30/70 monomer ratio)[40] at the indicated combinations of temperature and pressure demonstrating the invariance of the dispersion at constant value of the local segmental relaxation time. The ordinate scale for each curve has been shifted slightly to make the peak coincide at their maxima.

III. DIRECT MEASUREMENT AT HIGH RATES AND LARGE STRAINS

Beyond the inherent problems with extrapolating to high strain rates based on time-temperature superpositioning, the procedures in Section II usually involve linear viscoelastic measurements at small amplitudes. Thus, to obtain predictions about large strain behavior requires the assumption that the time-temperature shift factors are invariant to strain.[41-43] For properties such as the strength of rubber or orientational crystallization, low strain measurements are not obviously germane. Consequently, substantial effort has been expended over the years to obtain directly the mechanical properties of rubber at high rates and high strains. These methods, the primary ones being compression tests with a split Hopkinson bar apparatus and extension measurements using some variation on an impact test, are described below.

A potential problem with high speed testing of rubber is the generation of viscous heat. Stress/strain curves for rubber measured over a broad range of rates sometimes show unphysical effects, ascribed to a departure from isothermal conditions at high strain rates.[44-46] Thermal diffusivities for rubber are low (0.001 – 0.002 cm^2/s),[47] so that heat dissipation may be incomplete at best. Filled rubbers usually generate more heat although this is partly compensated for by better heat conduction, the diffusivity increasing in proportion to the carbon black concentration. Various experiments have found temperature rises in rubber samples during rapid stretching, beginning with the classic observations of Gough and Joule on natural rubber, wherein the heat rise is augmented by strain crystallization.[48] Mitchell and Meier[1] followed strain crystallization of stretched gum natural rubber by observing temperature increases in embedded thermocouples. Similar but more sensitive experiments by Glaser and Eirich[2] found measurable temperature rises for strain rates exceeding about 40 s^{-1}. Hauk and Neumann[44] stretched rubber to failure "in less than one second" and observed changes due to non-isothermal conditions. The extent of the departure from isothermal data depended on the degree of strain crystallization and the crosslink density of the test specimen. As a rule of thumb, high rate testing in which experiments are completed in tens of ms or less can be regarded as strictly adiabatic. For dynamic testing, conducted in the linear viscoelastic regime using small strains, the difference between the isothermal and adiabatic dynamic moduli of rubber is negligible.[9] For large strains, there is obviously greater heat generation; moreover, stretching an elastomer can decrease the diffusivity transverse to the strain direction.[49] However, since rubber properties are only weakly T-dependent (*i.e.*, the rubbery plateau modulus in Figure 3), even for large strains the difference between isothermal and adiabatic behavior may be minimal in the absence of crystallization. The exception would be rates that are fast enough to bring the rubber into the transition zone (see Section IV), in which temperature changes exert large effects on the modulus.

A. WAVE PROPAGATION

For testing at very fast speeds, wave propagation can influence the material response. When subjected to a mechanical perturbation, stress propagates through the material as a pressure wave, which is longitudinal in an "infinite medium" but also can be in the form of a shear wave, for example for transmission through a thin film. For the former, the propagation velocity, c, is given by[50]

$$c = \sqrt{V\left(K + \frac{4}{3}G\right)} \qquad (1)$$

where and K and G are the respective bulk and shear moduli (the bracketed quantity is referred to as the longitudinal modulus). For a typical rubber, the bulk sound speed c ≅ 1500 m/s. For

shear waves, the corresponding relation for a linear material is[50]

$$c = \sqrt{VG} \tag{2}$$

Equations (1) and (2) assume negligible damping (energy absorption). The bulk and shear modulus are related by

$$K = \frac{2(1+\nu)G}{3(1-2\nu)} \tag{3}$$

where ν is Poisson's ratio. For gum natural rubber, ν = 0.4999,[51] which means that pressure travels ~700 times faster as a longitudinal wave than as a shear wave. If the modulus decreases with strain, the stress wave is continuous and fans out through the material. However, at high strain rates the wave may lag behind the material displacement, so that equilibrium with respect to stress and strain is not immediately attained.

A modulus that is an increasing function of strain, as often the case for rubber at moderate to large strains, causes acceleration of the stress wave with the pulse becoming extended along the propagation direction. If the pulse moves faster than the speed at which the wave can propagate, the pulse front becomes progressively steeper, with the propagating waves ultimately collecting to form discontinuities. This condition, associated with very abrupt changes in density and pressure, is referred to as a "shock wave". The steep front characteristic of a shock wave is seen in Figure 14 for a stretched natural rubber. This wave character only becomes important for deformations that approach the velocity of sound, and a strain-hardening mechanical response is also necessary for the pulse speed to exceed the wave propagation speed. A related phenomenon is the upper limit for the velocity of cracks propagating in rubber, which is governed by the wave velocity.[3,52,53]

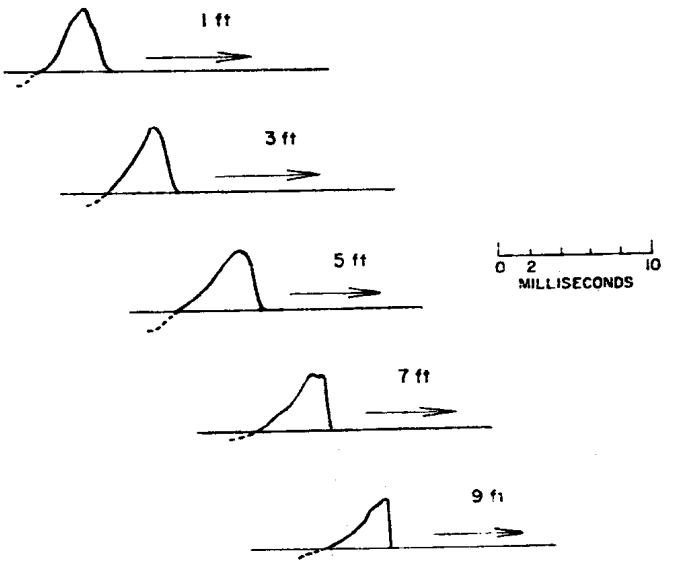

FIG. 14. – Velocity versus time measured on an unfilled NR vulcanizate extended to a strain of 440%. After propagating ~ 9 ft, the pulse assumes the appearance of a shock wave [from Ref. 68; reproduced with permission].

Since the velocity of a pressure pulse depends on the modulus of the medium (Equations (1) and (2)), measurement of the sound velocity can be used to determine the modulus. Sinha *et al.*[54] applied this technique to characterize the elastic properties of siloxane networks of varying crosslink density. Sonic (≤ 20 kHz) and ultrasonic (up to GHz) measurements have been used to determine the high frequency modulus of various polymeric materials.[55-57] Ultrasound techniques are common in medicine for characterizing the mechanical properties of tissue and bone,[58-61] although the frequency range is limited to < 15 MHz due to attenuation problems. Conventional experiments using sound waves only probe the linear mechanical response since the strain amplitudes are very low (≤ 10^{-6}).

An interesting variation is analysis of stress wave propagation in thin rubber strips either plucked[62] or allowed to retract freely from a state of tension.[63-65] The mode of propagation in a thin rod or plate is an extensional wave, since the local deformation is accompanied by lateral contraction. The velocity of an extensional pulse is related to the tensile modulus, E, by

$$c = \sqrt{VE} \tag{4}$$

For low rates (moderate strains) the wave travels with a constant velocity and the linear behavior is measured;[66] however, at higher extensions (a few hundred percent or more) the wave is dispersed, as the medium responses nonlinearly. The relevant modulus in Equation (4) is the differential modulus associated with the time- and position-dependent strain.[65] Mason[67] derived an expression whereby the stress/strain curve can be obtained from the velocity of an extensional wave in freely retracting rubber, using

$$E = m\left(\frac{dc}{d\varepsilon}\right)^2 \tag{5}$$

where ε is the strain and *m* the mass per unit length of the unstretched rubber. This offers a potential means to obtain data at high rates of strain, although the method is largely unexploited toward that end. Very high rates can produce a shock wave in the retracting rubber[68,69] (see Figure 14), an example of shock formation by an extensional wave.

The wave nature of stresses in rubber is manifested in the behavior of crack formation in highly stretched rubber.[53,70] Cracks exhibit an oscillatory nature when the crack propagation speed is very high.[71] The features are similar to shocks waves, with crack velocities observed to be intermediate between the longitudinal and shear wave speeds.[72]

B. SERVOHYDRAULIC TEST INSTRUMENTS

Servohydraulic systems, in which pressurized fluid drives the test assembly, are commercially available and can yield substantial displacements (~ 50 cm) even with stiff samples. Although speeds as high as *ca.* 25 m/s are attainable, these usually limit the displacement (< 5 cm). Even small displacements may correspond to large strains in compression tests, but generally the rates using servohydraulic instruments do not exceed 10 s^{-1}.[73,74] Nakajima and coworkers[41,42] obtained strain rates up to ~ 270 s^{-1} in experiments on rubber using a servohydraulic instrument, although the scatter in the data was large.[43]

C. SPLIT HOPKINSON BAR (SHB)

In the split Hopkinson bar experiment[75] a cylindrical sample is placed between the ends of two elastic bars (typically aluminum). A third, smaller "striker" bar is accelerated toward the

incident bar (see Figure 15) by means of pressurized gas or a pendulum. The reflected and transmitted pulses are measured, usually with strain gauges attached to the bars, and from these the properties of the sample are deduced. The test was originally developed for steel[76] but has been applied to a range of materials including polymers. The strain rate on the sample is given by[77]

$$\frac{d\varepsilon_r}{dt} = -\frac{2c}{l_s}\varepsilon_r(t) \tag{6}$$

in which ε_r is the reflected strain, l_s the undeformed sample length, and the incident longitudinal wave velocity c is given by Equation (1) using the known properties of the bar. Integration of Equation (6) yields the sample strain, while from continuity of the forces the stress is

$$\sigma(t) = \frac{A_t}{A_s}E_t\varepsilon_t(t) \tag{7}$$

where the ε_t is transmitted strain, E_t the modulus of the transmission bar, and A_t and A_s are the respective cross-sectional areas of the transmission bar and the sample. The operating assumption of the method is that the transmitted and reflected stress (strain) profiles sum to the incident pulse

$$\varepsilon_i = \varepsilon_r + \varepsilon_t \tag{8}$$

Some typical results are shown in Figure 16 for a filled polybutadiene elastomer.[78] As seen from Equation (6), higher strain rates require progressively thinner samples. This also serves to reduce signal attenuation due to damping of the wave amplitude by the rubber. Typically, thicknesses in the range 1.5 – 3 mm are used for rubber samples. In SHB testing the assumption is made that the sample remains a right cylinder, with grease often employed to facilitate sliding at the interface with the bars. In reality, it is very difficult to avoid barreling when a rubber cylinder is compressed,[79] so that without high speed photography, it is not obvious whether corrections for barreling of the test specimen are required.

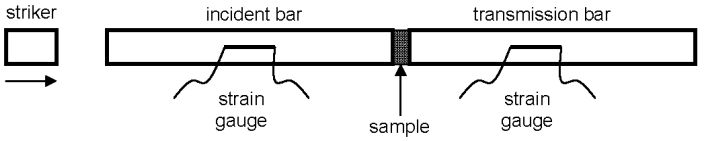

FIG. 15. – Schematic of a split Hopkinson bar instrument. The short striker bar impacts the incident bar, causing transmission of a compressive pulse to the sample, which is between the incident and transmission bars. Most of the pulse is reflected back with a small amplitude pulse passing through the sample into the transmission bar. The reflected and transmitted pulses in the two bars yield respectively the strain and stress in the sample.

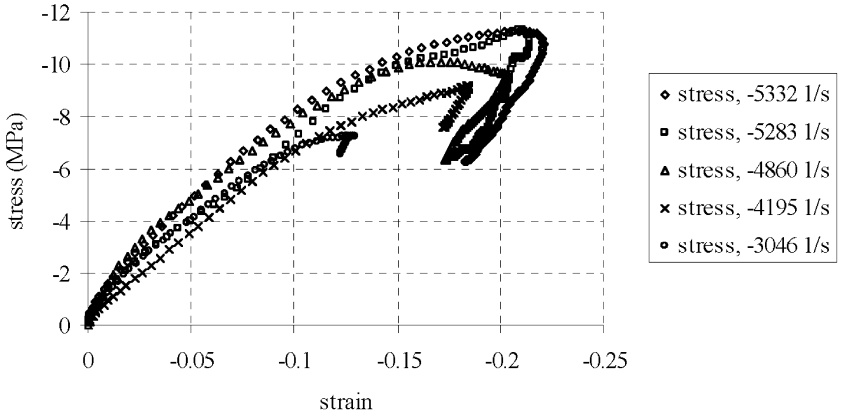

FIG. 16. – True stress *vs.* log strain for filled 1,4-polybutadiene compressed ~ 20% using a SHB instrument.[78]

The ratio of the amplitudes of the incident and reflected stress waves is related to the impedance difference between the bar, z_i, and sample, z_s

$$R = \frac{z_i - z_s}{z_i + z_s} \tag{9}$$

where z = c/V. Since the impedance of rubber is much less than that of a metal bar, little of the incident stress wave is transmitted through the sample, introducing large errors into the analysis. This can be compensated for in part by using a plastic (*e.g.*, polycarbonate) as the bar material.[80,81] The impedance of polycarbonate is about an order of magnitude smaller than aluminum and thus closer to that of the rubber (for which $z \sim 1.5\times10^6$ kg m^{-2} s^{-1}). An alternative approach is to place force transducers on the test specimen to directly measure the stresses on the sample.[82,83] Song and Chen[84] adopted this method to obtain results up to 4700 s^{-1} on an ethylene-propylene-diene terpolymer (EPDM) rubber (Figure 17). Direct force measurements have also shown that the two ends of a test specimen can have differences in pressure due to inertial forces and non-uniform deformation due to wave propagation (the stress pulse moves faster than the wave speed so that the initial material response is not at equilibrium). The magnitude of these errors depends on the sample length and the strain rate.[80,85]

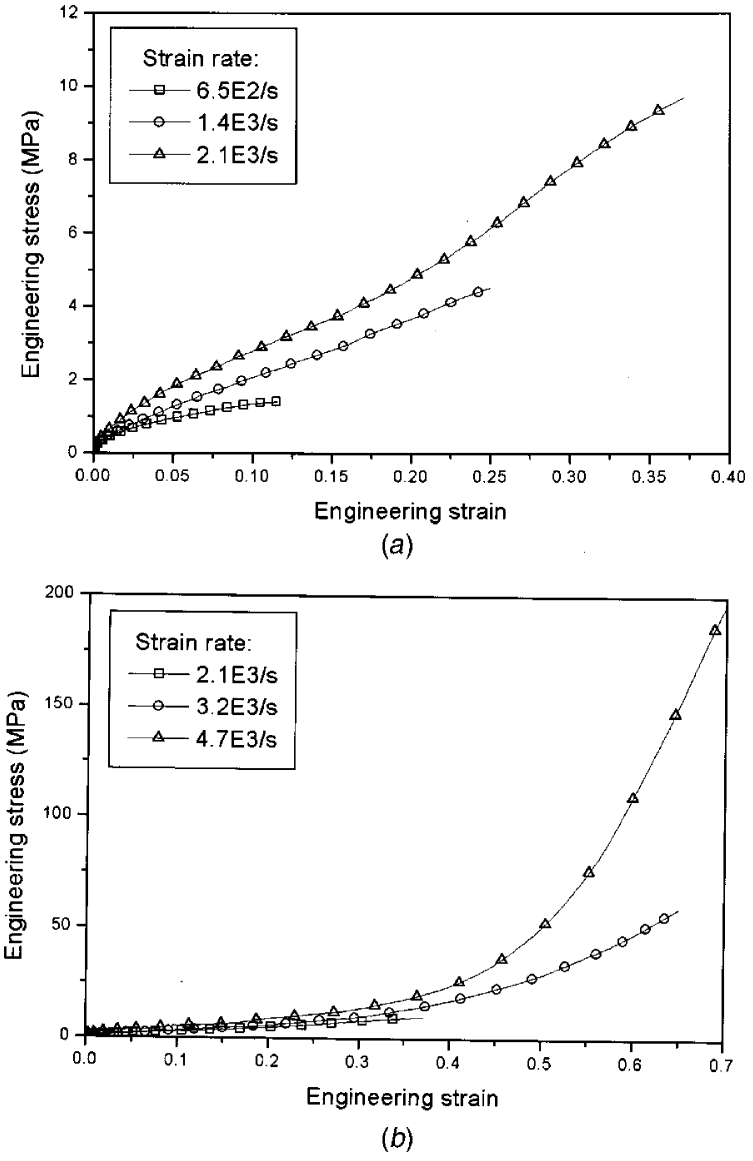

FIG. 17. – Compression stress/strain curves for EPDM rubber using a SHB instrument.[84]

Modifications of the SHB test have been introduced to enable tension data to be obtained, for example by used a clamping arrangement to convert the impact from the striker bar into a tensile force on the sample.[86] Shim *et al.*[81] carried out tensile measurements on silicone rubber, achieving an extensional strain rate of 1,200 s^{-1}. Rae and Brown[87] measured Teflon in tension at strain rates up to 800 s^{-1}.

D. DROP WEIGHT AND PENDULUM TESTERS

Whereas the SHB technique is well developed and almost a standard method to study the high speed compression of materials, methods to measure the extension of rubber at high rates are less common and very customized.

Albertoni[88] used a modified pendulum hammer, which stretched a ring test piece to a pre-

determined elongation at constant strain rates up to ~ 80 s^{-1}. Following release of the rubber sample at the bottom of its fall, the pendulum continues to a new height, as determined by the retained energy. The difference in the initial and follow-through heights of the pendulum yields the strain energy imparted to the rubber. A different test specimen was used for each point on the obtained stress/extension curve. A comparison of results for a gum vulcanizate at low and high strain rates is shown in Figure 18.

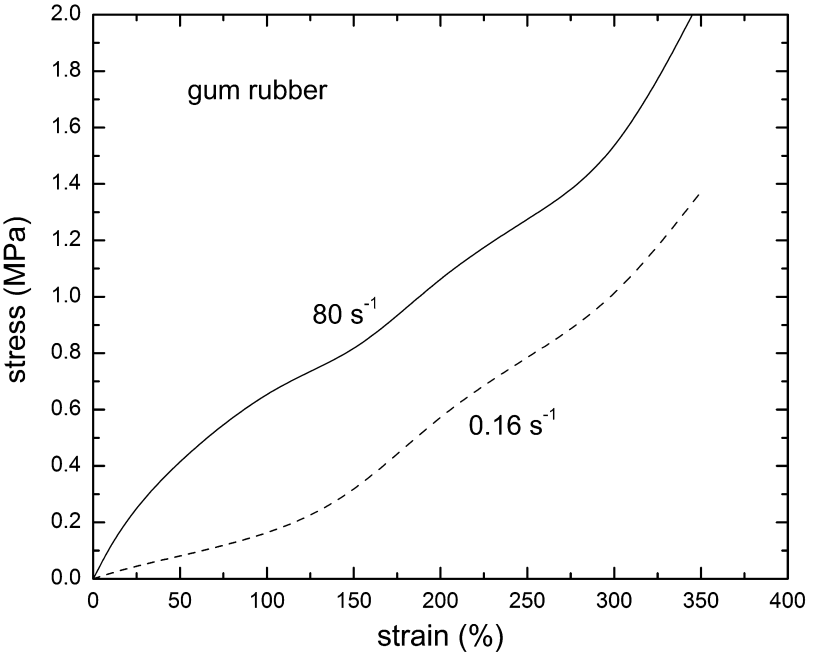

FIG. 18. – Extension stress/strain curves calculated from data for an unfilled (and unidentified) rubber.[88]

Roth and Holt[45] designed the first instrument employing a falling weight to achieve high strain rates. A rubber sample in the form of a ring was elongated at a non-uniform rate, increasing up to a maximum (of as high as 20 s^{-1}) roughly 2/3 of the way through the test, before decreasing to the point of failure. The stress/strain curves for high speed were generally above those for slow speed testing, although at very high elongations the curves sometimes crossed. This was ascribed to heating of the rubber specimen due to the adiabatic condition of the test.

Villars[46] achieved strain rates as high as 2,700 s^{-1} with an instrument employing a wheel rotating up to 1,700 rpm. A pin attached to the circumference of the wheel strikes a rubber sample in the form of a loop, causing it to stretch at a constant rate. A piezoelectric crystal was used to measure the stress. Stress/strain curves were reported for only one gum rubber, of unidentified composition. The stresses were lower at higher strain rates, suggesting adiabatic heating or some artifact in the experimental procedure. Plots of tensile strength versus strain rate showed minima for strain-crystallizing rubbers.

Compressive strain rates approaching 200 s^{-1} were achieved by Gale and Mills[89] with a falling weight apparatus. Integration of accelerometers attached to the weight was used to determine both the force and displacement of the foam test samples. Hoge and Rinde[90,91] obtained high speed stress/strain measurements on a polystyrene foam using a modified metal-working machine. The instrument uses compressed gas to rapidly expand a piston, achieving strain rates up to 100 s^{-1}. These data partly bridge the gap between conventional tests and SHB experiments

at 1,400 s^{-1}. As shown in Figure 19, at all rates the modulus in tension was consistently higher than in compression, with the latter showing negligible strain-rate dependence.[91]

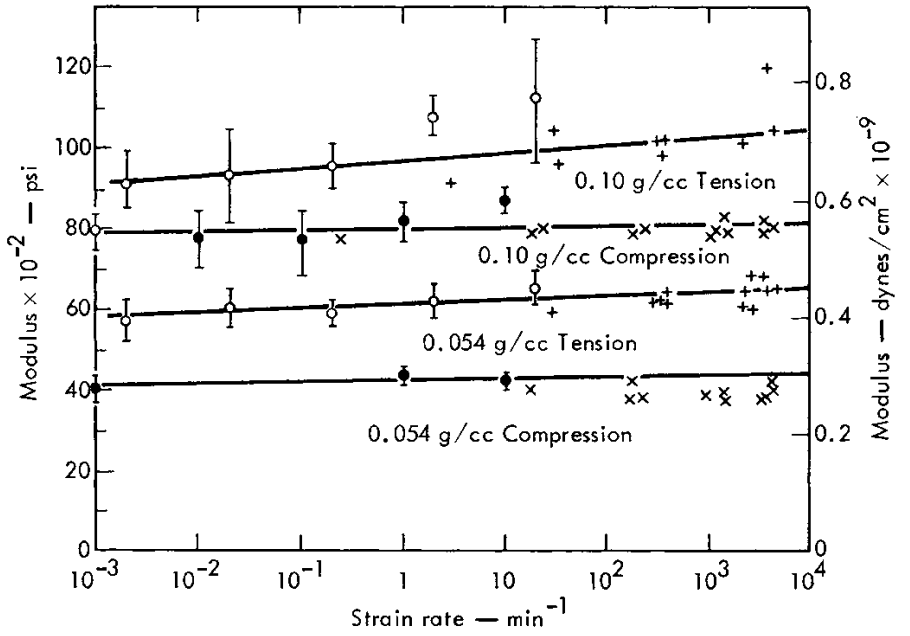

FIG. 19. – Tangent modulus measured on polystyrene foam samples having the indicated density as a function of strain rate in both tension (hollow symbols) and compression (filled symbols) [from Ref. 91; reproduced with permission)].

More recently Hoo Fatt and coworkers[92,93] have developed a high speed extension device based on a Charpy impact tester. By means of pulleys, the falling pendulum accelerates two slider bars attached to the sample, to achieve strain rates up to 480 s^{-1} depending on the drop height. The load is determined from strain gauges attached to the sample grips, and the strain is measured with linear variable displacement transducers (LVDT). Stress/strain curves for a styrene-butadiene copolymer (SBR) are shown in Figure 20.[93] Note that while the failure strain initially increases with strain rate, at higher rates it begins to decrease. Curiously, above strain rates of ~ 325 s^{-1}, the stress/strain curves becomes almost invariant to rate, other than a decrease of the failure strain. This is not seen in SHB compression data for rubber (*e.g.*, Figures 16 and 17).

An instrument incorporating many of the features of the Hoo Fatt design has been developed by Mott *et al.*[94] and is shown in Figure 21. It uses a falling weight in place of the pendulum and increases the slider velocity by using 4 : 1 lever arms to pull the cables. The strain is determined with a high speed camera, which can record over 100,000 frames per s.

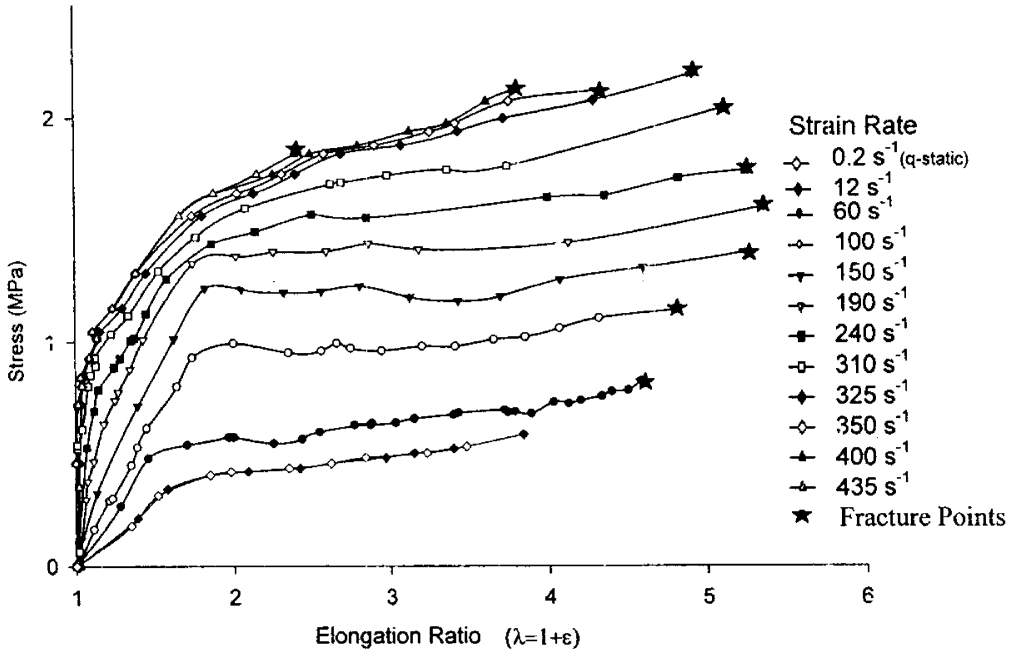

FIG. 20. – Tensile engineering stress *vs.* stretch ratio for an unfilled SBR at the indicated strain rates.[93]

One potential problem with high extension rate experiments is the contribution of inertia to the response. This is seen in the data in Figure 22[94] as a steep initial rise in the stress. By repeating the experiment in the absence of a sample, the inertial contribution is observed directly (Figure 23); it corresponds to the mass of the empty sample grips.

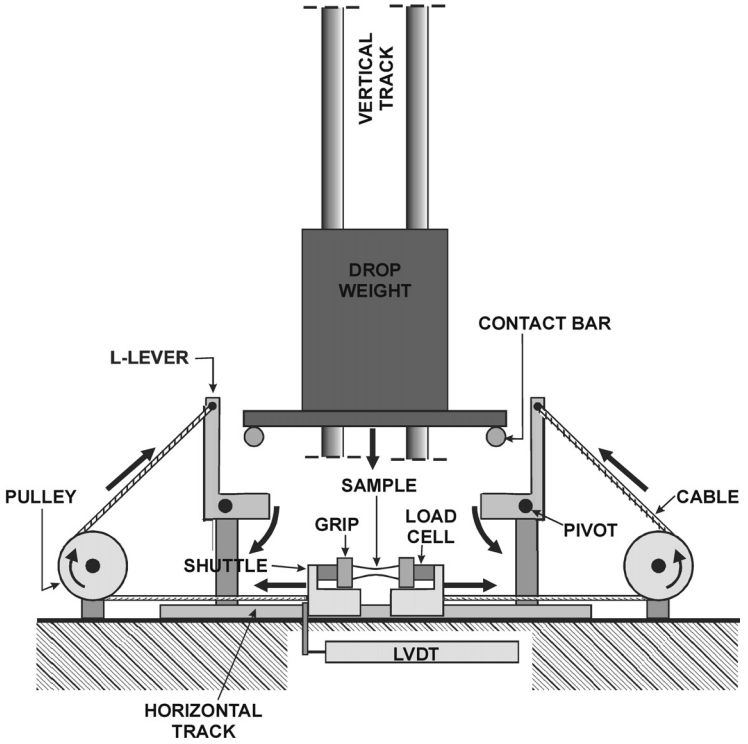

FIG. 21. – Schematic of tester (not to scale) employing a 100 kg weight dropped from a variable height.[94] The speed is controlled by the drop height (maximum = 4.6 m), which exerts tension on the cables via the lever arms. This causes motion of the shuttles to stretch the sample. The forces are measured with a load cell supplemented by piezoelectric strain gauges attached to the grips, with the strain determined using a high-speed camera; the LVDT is optional.

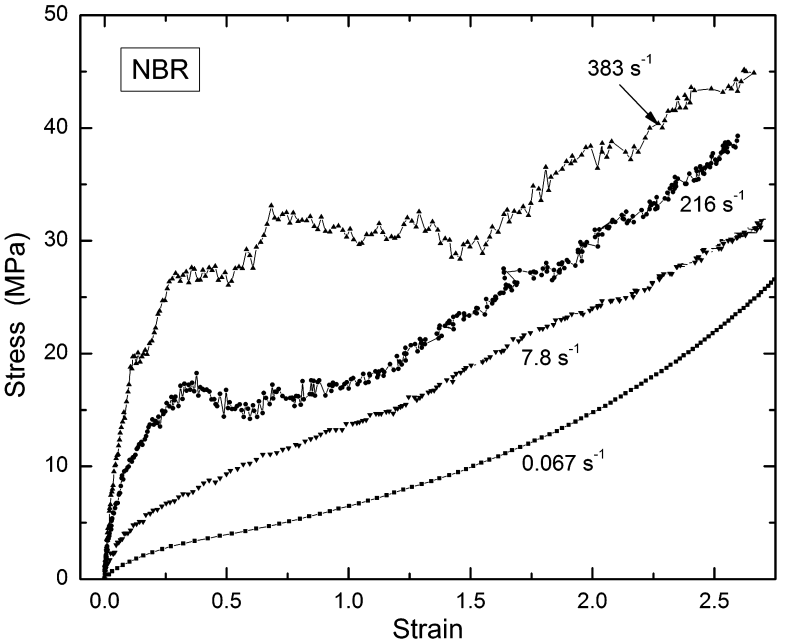

FIG. 22. – Stress/strain curves for a nitrile rubber at a conventional test rate and elongated at high rates using the instrument in Figure 21.[94]

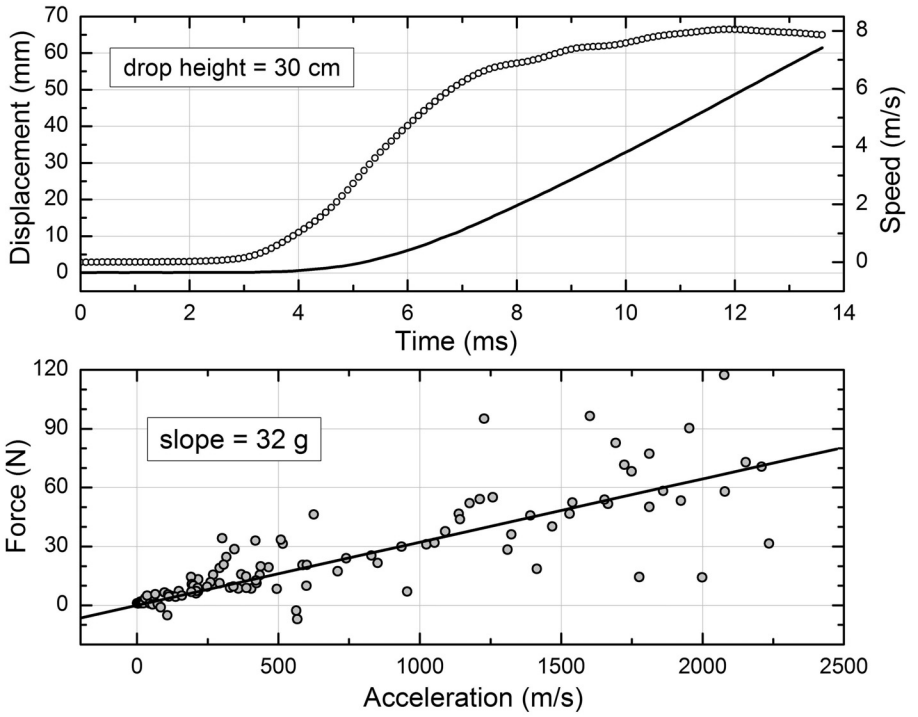

FIG. 23. – Force, displacement, acceleration, and load measured with the tester in Fig. 21 without a sample present. The inertial mass, 32 g, corresponds to that of the empty specimen holders.[94]

E. EXPANDING RING TECHNIQUE

A less common method of determining stress/strain properties at high rates is the freely expanding ring technique. The sample in the form of a thin ring is slipped over a hollow, thick-walled metal cylinder. The walls of the cylinder are rapidly expanded using either an electromagnetic pulse[95] or gas pressure generated inside the cylinder by an explosive charge or rapid vaporization of a wire subjected to a sudden high voltage.[96,97] The cylindrically symmetric expansion of the walls transfers momentum to the ring, causing it to move away from the tube. The deformation state of the sample is uniaxial tension provided the ring thickness is no more than 5% of its diameter. High speed photography is used to measure the sample radius, r, as a function of time. The true stress, true strain, and the strain rate are then determined as[98]

$$\sigma = -\frac{r}{V}\frac{\partial^2 r}{\partial t^2} \tag{10}$$

$$\varepsilon(t) = 1n\left(r(t)/r_{t=0}\right) \tag{11}$$

and

$$\frac{\partial \varepsilon}{\partial t} = \left(\frac{\partial r}{\partial t}\right)/r \tag{12}$$

Strain rates exceeding 10^4 s^{-1} can be achieved; however, the rate is not constant but decreases continually to zero over the course of the experiment. Figure 24 shows data for an ultra-high-molecular-weight polyethylene (UHMWPE), along with SHB data. The latter approach the curve for the expanding ring measurements as the strain rates become nearly the same.

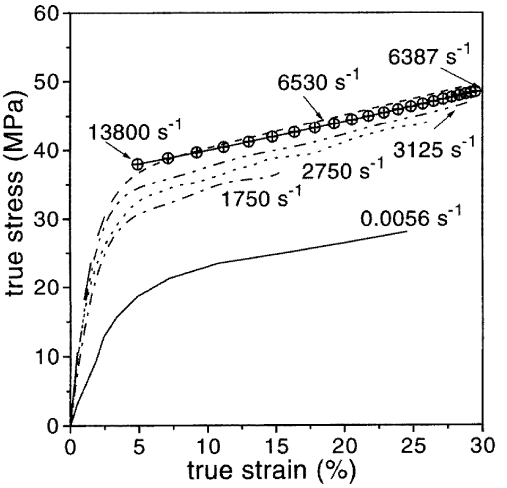

FIG. 24. – Comparison of stress/strain curves for an UHMWPE sample tested in quasi-static compression (solid line), SHB compression (broken lines), and in tension using the expanding ring technique (symbols) [from ref. 96, reproduced with permission].

F. CATAPULT APPARATUS

Large stretching rates in rubber have been achieved with a catapult device using either a steel spring[44] or rubber bands.[99,100] For the latter, the mechanical energy stored in the stretched rubber bands (not the test specimen) is released to accelerate weights on a guide rail. The moving weights displace the rubber test sample at a constant speed. Velocities of 18 m/s have been achieved, corresponding to strain rates approaching 200 s^{-1}.[100] However, this design has only been employed for strength testing of rubber, without any measurements of stress/strain curves. Such an instrument can be constructed to be more compact than falling weight and other impact devices, by taking advantage of the enormous energy storage capacity of elastomers.[101]

IV. STRAIN-INDUCED GLASS TRANSITION

Deformation-induced transitions in materials are well-known. Strain-crystallization of natural rubber is the source of its exceptional mechanical properties and has been the subject of many studies.[102-107] The possibility also exists for a change in the phase morphology of multi-component rubbers due to strain.[108,109] These phenomena are not unique to elastomers: metal alloys[110] and ceramics[111] undergo solid-solid phase transitions as a result of mechanical stress. The effect serves as the mechanism for many shape-memory materials.[112] The glass transition is usually effected by cooling. However, since T_g is effectively the temperature at which the material response time becomes longer than the experimental time scale (as molecules become too slow in attaining their dynamic equilibrium configurations), high strain rates can induce a transition to the glassy state even at temperatures well above the conventional T_g. As measured by calorimetry or volumetrically, T_g corresponds to the temperature at which the segmental relaxation time is in the range from 10 – 10,000 s.[24,113] (Interestingly, when T_g is changed by varying the pressure, for example in a PVT experiment, the characteristic value of the relaxation time at

$T_g(P)$ remains constant.)[24]

The glass transition is associated with the largest mechanical hysteresis, and this high damping is exploited in various applications of rubbery materials. A few examples are described below, all having in common that the rubber is deformed fast enough for the response to involve the transition zone of the viscoelastic spectrum. In this regard, we note there is a transition observed in tear tests on rubber carried out at high crack propagation rates (~ 1 mm/s), which is associated with development of a smooth crack interface; however, this phenomenon apparently does not involve the onset of the glass transition.[3,114,115]

A. WET SKID RESISTANCE OF TIRES

Surface conditions exert a dominant role on the friction of rubber,[116,117] the friction coefficient varying by four orders of magnitude depending on the interface.[118] Adhesive forces (primarily van der Waals bonding) contribute to the friction of rubber on dry and very smooth surfaces. On wet or rough surfaces, bulk energy dissipation becomes dominant as the rubber is deformed by surface asperities, which usually range in size from 0.01 to 1 mm.[119] This mechanical hysteresis of the rubber governs the friction of sliding tires[120-122] and obviously is related to the material properties; that is, it is not a surface property. (An exception might be sliding on ice, for which the nature and behavior of the ice surface can be significant.[123-125]) During sliding on a wet surface, anti-lock braking systems increase the contribution from surface adhesion, which otherwise is negligible. Persson has suggested that wet sliding reduces the contact area of the tread, with pooled water serving to isolate the tread from the high frequency deformations caused by road asperities.[122]

Since wet skid resistance is determined by the amount of energy dissipated in the rubber, the response of optimal tread compounds should fall within the transition zone, where hysteresis is maximum. The frequency associated with wet skidding is in the range from 10^3 to 10^6 Hz;[126,127] thus, rubbers having high glass transition temperatures are expected to have superior wet skid resistance. However, since T_g as conventionally measured corresponds to low frequencies (≤ 0.1 s^{-1}) and extrapolation of time-temperature shift factors is ambiguous (Section II A), deviations from a correlation between T_g and wet skid resistance are expected and have been reported.[128,129] Figure 25 shows laboratory wet skid resistance of various elastomers as a function of T_g. Butyl rubber is an outlier when T_g is measured calorimetrically, but has the expected behavior when T_g is measured using NMR, for which the relevant frequency is much higher (~ 10^4 s^{-1}).[129] Takino *et al.*[128] reported good correlation of wet skid behavior with the temperature of the peak of the mechanical loss tangent measured at 10 Hz (Figure 26). Since this is lower than the skidding frequency, it still involves extrapolation and thus may not always be accurate.

B. SOUND TRANSMISSION AND DAMPING

Rubber finds various uses in acoustics, including decouplers, which prevent sound passage, anechoic coatings, which attenuate sound reflections, and acoustic windows, which transmit sound waves. Although commercial materials are usually proprietary, compilations of acoustic properties for many elastomers have been published.[130] One important property is the attenuation of sound as it passes through an elastomer. The diminution of the sound pressure, p, is quantified by the attenuation coefficient, α, a material property defined as $\alpha \equiv \frac{-dp/p_0}{dx}$ where p_0 is the initial pressure and x the propagation distance. For small values of the loss tangent[9]

$$\alpha = \frac{\pi \tan \delta}{\lambda} \quad (\alpha << 1) \tag{13}$$

For longitudinal waves (oscillating in the direction of the sound propagation), the loss tangent in Equation (13) refers to the bulk modulus, which for rubbers is quite small ($<10^{-3}$.)[9]

When sound damping is the objective, longitudinal waves can be converted into shear waves,[50] for which loss tangents are larger. The greatest attenuation will be achieved if tan δ is maximized by ensuring that the elastomer undergoes its rubber-to-glass transition at the sonic frequency. As a result the selection of damping materials, such as coatings used on Navy vessels for sonar attenuation, is often governed primarily by their T_g. The objective is to have the peak of the loss tangent centered within the sound frequencies at the operating temperature (*e.g.,* -2 °C to 38 °C for sea water). Variation of the latter means that a broad glass transition is desirable and has led to the use of blends and polyurethane materials for many naval applications.[50] These same consideration apply to vibration isolation systems – rubber having a large and broad loss tangent most effectively suppresses the transmitted forces.[131,132]

C. IMPACT PROTECTION

A recent development in military technology, spurred by the rise of Islamic terrorism, is the use of rubber coatings for protection from ballistic and explosive assault.[133] Elastomeric coatings on vehicles and buildings minimize damage to the underlying structure and collateral damage from fragmentation. Most current applications involve polyureas, which can be applied as spray-on coatings to buildings and vehicles. Polyureas are formed from the reaction of isocyanates with polyetheramines, which occurs very fast (gel times < one minute), so that formation of the coating is independent of ambient temperature and humidity. The extensive hydrogen-bonding of polyureas yields good mechanical properties (high modulus and high elongation).

The U.S. Air Force and Army have coated the walls of various buildings and trailers with polyurea.[134,135] The coating adheres to the structure (*e.g.*, cinder block, concrete foundation, or wood beams) and remains intact when subjected to a bomb blast. The principle function of the coating is to reduce fragmentation of the underlying structure. Debris propelled by the blast pressure can attain high speeds (thousands of feet per second) and is a leading cause of injury from terrorist bombings. The main requirements of these rubber coatings are that they adhere to the structure and remain intact when elongated at very high rates. Since mitigating the blast pressure is not the specific objective, energy damping in the coating, and any contribution therein from a pressure induced glass transition, is not a primary consideration.

The U.S. Navy has also used polyurea coatings in an effort to directly mitigate damage from gunfire and bombs to the High Mobility Multipurpose Wheeled Vehicle (HMMWV) and other light duty vehicles.[133,136,137] These polyurea coatings (referred to as "DragonShield")[138] are considerably more compliant than those used on buildings (at least when tested at conventional laboratory rates). Extensive tests have demonstrated their effectiveness, although the mechanism for the blast mitigation is uncertain, with shock wave interference phenomena suggested as one contributing factor.[139] Since ballistic impact deforms the target surface very rapidly (approaching MHz frequencies), a contribution from a stress-induced glass transition with consequent energy dissipation is possible. Impact testing has shown some correlation between T_g and performance similar to that seen in Figure 25 for wet skid resistance.[140]

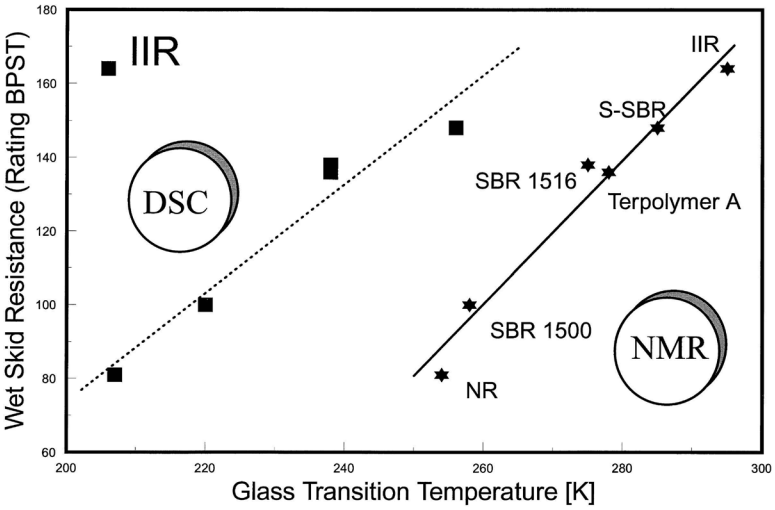

FIG. 25. – Wet skid resistance measured on the British Pendulum Skid Tester (BPST) versus glass transition temperature, the latter measured by differential calorimetry and by NMR.[129]

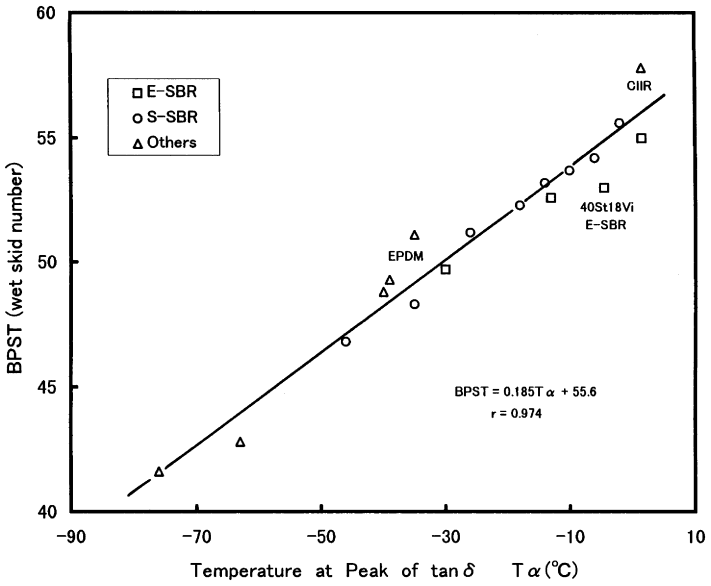

FIG. 26. – Laboratory skid resistance versus the temperature of the maximum in the mechanical loss tangent measured at 10 Hz for rubbers having T_g's (measured by DSC) from -106 to -20 °C.[128]

V. SUMMARY

When the mechanical properties of rubber at high strain rates are deduced from conventional dynamic measurements using the time-temperature superposition principle, it is critical that the shift factors used for the extrapolation correspond to the same mode (segmental or terminal) as that of the mechanism of interest. Otherwise there is the potential for large errors since these modes can have quite different temperature dependences. There remains the problem of predicting large strain behavior from small strain measurements. Since most data are obtained for ambient pressure, scaling methods can be employed to calculate the response at higher pressures.

These are well-established methods for data in the linear viscoelastic regime, although the accuracy for high strains has not been verified.

Direct determination of stress/strain curves for rubber at high strains (tension or compression) and high strain rates can be accomplished by a variety of methods, virtually all of which involve custom-made instrumentation. Problems with these methods include non-constant strain rates, non-isothermal conditions, wave effects and (related) departures from stress equilibrium. Nevertheless a fair number of data have been published, indicating the feasibility of such tests.

While there are many applications involving rubber subjected to high strain rates, only three are reviewed herein. These have in common that the deformation of the rubber can cause its transition to the glassy state. This transition promotes large energy dissipation and thus can be exploited for wet skid resistance in tires, acoustic attenuation, and coatings for impact protection.

VI. ACKNOWLEDGEMENTS

I thank C. G. Robertson and P. H. Mott for useful comments. This work was supported by the Office of Naval Research.

VII. REFERENCES

[1]J. C. Mitchell and D. J. Meier, *J. Polym. Sci. A2* **6**, 1689 (1968).

[2]Z. R. Glaser and F. R. Eirich, *J. Polym. Sci. C* **31**, 275 (1970).

[3]G. J. Lake, C. C. Lawrence, and A .G. Thomas, RUBBER CHEM. TECHNOL. **73**, 801 (2000).

[4]E. R. Fitzgerald and R. E. Fitzgerald, *Polym. Bull. (Berlin)* **18**, 167 (1987).

[5]M. Mareanukroh, R. K. Eby, R. J. Scavuzzo, and G. R. Hamed, RUBBER CHEM. TECHNOL. **73**, 912 (2000).

[6]M. Mareanukroh, G.R. Hamed, and R. K. Eby, RUBBER CHEM. TECHNOL. **69**, 801 (1996).

[7]M. R. VanLandingham, S. H. McKnight, G. R. Palmese, R. F. Eduljee, J. W. Gillespie, Jr., and R. L. McCullough, *J. Mater. Sci. Lett.* **16**, 117 (1997).

[8]E. Dupas, G. Gremaud, A. Kulik, J.-L. Loubet, *Rev. Sci. Instr.* **72**, 3891 (2001).

[9]J. D. Ferry, "Viscoelastic Properties of Polymers," 3rd edition, Wiley, New York (1980).

[10]A.V. Tobolsky and R. D. Andrews, *J. Chem. Phys.* **13**, 3 (1945).

[11]T. L. Smith, RUBBER CHEM. TECHNOL. **51**, 225 (1978).

[12]K. A. Grosch, RUBBER CHEM. TECHNOL. **37**, 386 (1964).

[13]P. G. Santangelo and C. M. Roland, *Macromolecules* **31**, 3715 (1998).

[14]C. K. Hall and E. Helfand, *J. Chem. Phys.* **77**, 3275 (1982).

[15]K. L. Ngai and R. W. Rendell, *J. Non-Cryst. Solids* **131**, 942 (1991).

[16]D. J. Plazek, *J. Phys. Chem.* **69**, 3480 (1965).

[17]K. L. Ngai and D. J. Plazek, RUBBER CHEM. TECHNOL. **68**, 376 (1995).

[18]M. Doi and S. F. Edwards, "The Theory of Polymer Dynamics"; Oxford, Clarendon (1986).

[19]A. Schonhals, *Macromolecules* **26**, 1309 (1993).

[20]C. M. Roland, K. L. Ngai, P. G. Santangelo, X. H. Qiu, M. D. Ediger, and D. J. Plazek, *Macromolecules* **34**, 6159 (2001).

[21]D. J. Plazek, I. C. Chay, K. L. Ngai, and C. M. Roland, *Macromolecules* **28**, 6432 (1995).

[22]P. G. Santangelo, K. L. Ngai, and C. M. Roland, *Macromolecules* **26**, 2682 (1993).

[23]Marvin, R. S. in "Proceedings of the Second International Congress on Rheology," W. Harrison, Ed., Butterworths, London (1953), Vol. 6, p. 156.

[24]C. M. Roland, S. Hensel-Bielowka, M. Paluch and R. Casalini, *Rep. Prog. Phys.* **68**, 1405 (2005).

[25]R. Casalini and C. M. Roland, *Phys. Rev. E* **69**, 062501 (2004).

[26] R. Casalini and C. M. Roland, *Colloid Polym. Sci.* **283**, 107 (2004).

[27]C. M. Roland and R. Casalini, *J. Non-Cryst. Solids* **251**, 2581 (2005).

[28]C. M. Roland, J. L. Feldman, and R. Casalini, *J. Non-Cryst. Solids*, in press (cond-mat/0602132).

[29]R. Casalini, V. Mohanty and C. M. Roland, *J. Chem. Phys*., in press (cond-mat/0605304).

[30]G. Floudas and T. Reisinger, *J. Chem. Phys.* **111**, 5201 (1999).

[31]K. L. Ngai, R. Casalini and C.M. Roland, *Macromolecules* **38**, 4363 (2005).

[32]R. Casalini and C. M. Roland, *Macromolecules* **38**, 1779 (2005).

[33]C. M. Roland, R. Casalini, and M. Paluch, *J. Polym. Sci. Polym. Phys. Ed.* **42**, 4313 (2004).

[34]R. Casalini and C. M. Roland, *Phys. Rev. B* **71**, 014210 (2005).

[35]M. Paluch, C.M. Roland and S. Pawlus, *J. Chem. Phys.* **116**, 10932 (2002).

[36]C. M. Roland, R. Casalini, and M. Paluch, *Chem. Phys. Lett.* **367**, 259 (2003).

[37]C. M. Roland, M. Paluch, S. J. Rzoska, *J. Chem. Phys.* **119**, 12439 (2003).

[38]K. L. Ngai, R. Casalini, S. Capaccioli, M. Paluch and C. M. Roland, *J. Phys. Chem. B* **109**, 17356 (2005).

[39]C. M. Roland, R. Casalini, P.G. Santangelo, M. Sekula, J. Ziolo and M. Paluch, *Macromolecules 36*, 4954 (2003).

[40]S. H. Zhang, R. Casalini, J. Runt, and C.M. Roland, *Macromolecules* **36**, 9917 (2003).

[41]N. Nakajima, H.H. Bowerman, E.A. Collins, RUBBER CHEM. TECHNOL. **46**, 417 (1973).

[42]H. H. Bowerman, E. A. Collins, and N. Nakajima, RUBBER CHEM. TECHNOL. **47**, 307 (1974).

[43]N. Nakajima and E. Harrell, RUBBER CHEM. TECHNOL. **56**, 1019 (1983).

[44]V. Hauk and W. Neumann, RUBBER CHEM. TECHNOL. **12**, 64 (1939).

[45]F. L. Roth and W. L. Holt, RUBBER CHEM. TECHNOL. **13**, 348 (1940).

[46]D. S. Villars, *J. Appl. Phys.* **521**, 565 (1950).

[47]E. Camano, N. Martire, S.N. Goyanes, A.J. Marzocca, and G.H. Rubiolo, *J. Appl. Polym. Sci.* **63**, 157 (1997).

[48]J. P. Joule, *Trans. R. Soc. (London)* **149**, 91 (1859).

[49]A.W. Broerman, D.C. Venerus, and J.D. Schieber, *Int. J. Thermoplast.* **22**, 1215 (1999).

[50]"Sound and Vibration Damping with Polymers," R.D. Corsaro and L.H. Sperling, Eds., *ACS Symp. Ser.* **424**, Amer. Chem. Soc., Washington DC, 1990.

[51]M. A. Anderson, P. H. Mott, and C.M. Roland, RUBBER CHEM. TECHNOL. **77**, 293 (2004).

[52]N. F. Mott, *Engineering* **165**, 16 (1948).

[53]A. Stevenson and A. G. Thomas, *J. Phys. D Appl. Phys.* **12**, 159, 2101 (1979).

[54]M. Sinha, B. Erman, J.E. Mark, T. H. Ridgway, and H. E. Jackson, *Macromolecules* **36**, 6127 (2003).

[55]I. Alig, D. Lellinger, and S. Tadjbakhsch, *Polym. Mater. Sci. Eng.* **79**, 31 (1998).

[56]P. H. Mott, C. M. Roland, and R. D. Corsaro, *J. Acoust. Soc. Amer.* **111**, 1782 (2002).

[57]C. M. Roland and G. F. Lee, RUBBER CHEM. TECHNOL. **63**, 554 (1990).

[58]H. Hasan and P. Mason, *Phys. Med. Biol.* **23**, 917 (1978).

[59]G. H. Brandenburger, *Calcif. Tissue Int.* **53**, S151 (1993).

[60]N. R. Miller and J. C. Bamber, *Phys. Med. Biol.* **45**, 2057 (2000).

[61]E. Konofagou, J. Thierman, K. Hynynen, *Ultrasonics* **41**, 337 (2003).

[62]J. L. Wegner and J. B. Haddow, *J. Appl. Mech.* **57**, 667 (1990).

[63]R. B. Stambaugh, M. Rohner, and S.D. Gehman, *J. Appl. Phys.* **15**, 740 (1944.)

[64]B.A. Mrowes, S. L. Dart, and E. Guth, *J. Appl. Phys.* **16**, 8 (1945).

[65]A. N. Gent and P. Marteny, *J. Appl. Phys.* **53**, 6069 (1982).

[66]H. M. James and E. Guth, *J. Appl. Phys.* **16**, 643 (1945).

[67]P. Mason, *Proc. R. Soc. London, Ser. A* **272**, 315 (1963).

[68]H. Kolsky, *Nature* **234**, 1301 (1969).

[69]J. K. Knowles, *SIAM J. Appl. Math.* **62**, 1153 (2002).

[70]M. Marder, *Phys. Rev. Lett.* **94**, 048001 (2005).

[71]R. D. Deegan, P. J. Petersan, M. Marder, H. L. Swinney, *Phys. Rev. Lett.* **88**, 014304 (2002).

[72]P. J. Petersan, R. D. Deegan, M. Marder, H.L. Swinney, *Phys. Rev. Lett.* **93**, 015504 (2004).

[73]E. Arruda, Y. Wang, and P. Przbylo, RUBBER CHEM. TECHNOL. **74**, 560 (2001).

[74]J. S. Bergstrom and M. C. Boyce, *J. Mech. Phys. Solids* **46**, 931 (1998).

[75]H. Kolsky, *Proc. Phys. Soc. London B* **62**, 676 (1949).

[76]B. Hopkinson, *Philos. Trans. R. Soc. London, Ser. A* **213,** 437 (1914).

[77]S. Nemat-Nasser, J. B. Isaccs, and J. E. Starrett, *Proc. Math. Phys. Sci.* **435**, 371 (1991).

[78]S. J. Quintavalla and S. H. Johnson, RUBBER CHEM. TECHNOL. **77**, 972 (2004).

[79]P. H.Mott and C. M. Roland, RUBBER CHEM. TECHNOL. **68**, 739 (1995).

[80]L. Wang, K. Labibes, Z. Azari, and G. Pluvinage, *Int. J. Impact Eng.* **15**, 669 (1994).

[81]V. P. W. Shim, L. M. Yang, C. T. Lim, P. H. Law, *J. Appl. Polym. Sci.* **92**, 523 (2004).

[82]J. A. Rinde and K. G. Hoge, *J. Appl. Polym. Sci.* **15**, 1377 (1971).

[83]W. P. Rogers and S. Nemat-Nasser, *J. Amer. Cer. Soc.* **73**, 136 (1990).

[84]B. Song and W. Chen, *Trans. ASME* **125**, 294 (2003).

[85]X. J. Wu and D. A. Gorham, *J. Phys. IV* **7**, 91 (1997).

[86]S. Nemat-Nasser, J. B. Isaccs, and J. E. Starrett, *Proc. Math. Phys. Sci.* **435**, 371 (1991).

[87]P. J. Rae and E. N. Brown, *Polymer* **46**, 8128 (2005).

[88]G. J. Albertoni, RUBBER CHEM. TECHNOL. **10**, 317 (1937).

[89]A. Gale and N.J. Mills, *Plast. Rubber Process Appl.* **5**, 101 (1985).

[90]K. G. Hoge and R. J. Wasley, *J. Appl. Polym. Sci. Appl. Polym. Symp.* **12**, 97 (1969).

[91]J. A. Rinde and K. G. Hoge, *J. Appl. Polym. Sci.* **15**, 1377 (1971).

[92]M. S. Hoo Fatt and I. Bekar, *J. Mater. Sci.* **39**, 6885 (2004).

[93]I. Bekar, M. S. Hoo Fatt, and J. Padovan, *Tire Sci. Technol.* **30**, 45 (2002).

[94]P. H. Mott, D. F. Roland, H. Schrader, and C.M. Roland, to be published.

[95]W. H. Gourdin, S. L. Weinland, and R. M. Boling, *Rev. Sci. Instrum.* **60**, 427 (1989).

[96]N. S. Al-Maliky and D. J. Parry, *Meas. Sci. Technol.* **7**, 746 (1996).

[97]N. S. Al-Maliky and D. J. Parry, *J. Phys. IV* **4**, 71 (1994).

[98]C. R. Hoggat and R. F. Recht, *Exp. Mech.* **9**, 441 (1969).

[99]A. Chiesa, *Kautch. Gummi* **11**, WT161 (1958).

[100]P. Kainradl and F. Handler, RUBBER CHEM. TECHNOL. **33**, 1438 (1960).

[101]I. S. Choi, C. M. Roland, and L. C. Bissonnette, RUBBER CHEM. TECHNOL. **67**, 892 (1994).

[102]J. Gough, *Proc. Lit. Philos. Soc. Manchester, 2nd Ser.* **1,** 288 (1805).

[103]A. N. Gent, *Trans. Faraday Soc.* 50, 521 (1954).

[104]E. H. Andrews, P. G. Owen, and A. Singh, *Proc. R. Soc. London A* **324**, 79 (1971).

[105]C. M. Roland and M. L. Warzel, RUBBER CHEM. TECHNOL. **63**, 285 (1990).

[106]I. S. Choi and C. M. Roland, RUBBER CHEM. TECHNOL. **70**, 202 (1997).

[107]S. Toki, I. Sics, S. Ran, L. Liu, and B. S. Hsiao, *Polymer* **44**, 6003 (2003).

[108]G. R. Hamed, C.-H. Shieh, and D. N. Schulz, *Polym. Bull.* **9**, 525 (1983).

[109]C. M. Roland, G. G. A. Bohm, and P. Sadhukhan, *J. Appl. Polym. Sci.* **30**, 2021 (1985).

[110]J. C. Escobar and R. J. Clifton, *SPIE*, **2424**, 186 (1995).

[111]H. Tan and T. J. Ahrens, *J. Appl. Phys.* **67**, 217 (1990).

[112]J. K. Knowles, *Comput. Mech.* **22**, 429 (1999).

[113]C. A. Angell in "Relaxation in Complex Systems," K.L. Ngai and G.B. Wright, Eds., Natl. Tech. Info. Service, Springfield, VA (1984).

[114]K. Tsunoda, J. J. C. Busfield, C. K. L. Davies, and A. G. Thomas, *J. Mater. Sci.* **35**, 5187 (2000).

[115]G. Carbone and B.N.J. Persson, *Phys. Rev. Lett.* **95**, 114301 (2005).

[116]E. M. Bevilacqua and E. M. Percaprio, RUBBER CHEM. TECHNOL. **41**, 843 (1968).

[117]B. E. Sabey and G. N. Lupton, RUBBER CHEM. TECHNOL. **37**, 878 (1964).

[118]A. D. Roberts, *Tribiology Int.* **4**, 115 (1977).

[119]B. N. J. Persson, *Surf. Sci.* **401,** 445 (1998).

[120]G. Heinrich, RUBBER CHEM. TECHNOL. **70**, 1 (1997).

[121]M. Kluppel and G. Heinrich, RUBBER CHEM. TECHNOL. **73**, 578, 2000.

[122]B.N.J. Persson, U. Tartaglino, O. Albohr, and E. Tosatti, *Phys. Rev. B* **71**, 035428 (2005).

[123]S. Futamura, RUBBER CHEM. TECHNOL. **69**, 648 (1996).

[124]A. Ahagon, T. Kobayashi, T. Kobayashi, and M. Misawa, RUBBER CHEM. TECHNOL. **61**, 14 (1988).

[125]A. D. Roberts, *J. Adhes.* **13**, 77 (1981).

[126]R. Bond, G.F. Morton, and L.H. Krol, *Polymer* **25**, 132 (1984).

[127]R. R. Rahalkar, RUBBER CHEM. TECHNOL. **62**, 246 (1989).

[128]H. Takino and R. Nakayama, Y. Yamada, S. Kohjiya, and T. Matsuo, RUBBER CHEM. TECHNOL. **70**, 584 (1997).

[129]G. Heinrich and H. B. Dumler, RUBBER CHEM. TECHNOL. **71**, 53 (1998).

[130]R. N. Capps, "Elastomeric Materials for Acoustical Applications," Naval Research Laboratory, Washington DC (1989).

[131]R. N. Capps, RUBBER CHEM. TECHNOL. **59**, 103 (1986).

[132]J. C. Snowdon, "Vibration and Shock in Damped Mechanical Systems," Wiley, NY (1968).

[133]C. M. Roland in "Rubber Technologist's Handbook", Vol. 2, RAPRA, Shrewsbury, UK (2006).

[134]K. J. Knox, M. I. Hammons, T. T. Lewis, and J. R. Porter, "Polymer Materials for Structural Retrofit," *Air Force Research Laboratory Technical Report* (2001).

[135]J. S. Davidson, J. R. Porter, R. J. Dinan, M. I. Hammons, and J. D. Connell, *J. Perf. Constr. Fac.* **18**, 100 (2004).

[136]C. Holtzman, *New Mexico Business Weekly*, Dec. 27 (2004); www.ara.com/whatnew/lead/dragonshield/dragonshield_nmbizweekly_12-24-04.pdf

[137]A. Webb, *Albuquerque Journal*, Jan. 10 (2005); www.ara.com/whatnew/lead/dragonshield/dragonshield_abqjrnl_1-10-05.pdf

[138]www.specialty-products.com/pdf%20files/Tech%20Data/Dragonshield.pdf

[139]P. Toensmeier, *Defense Tech. Int.* Sept./Oct., (2005), p. 18.

[140]C. M. Roland, unpublished.

[*Received March 2006, revised June 2006*]